Evaluation of a fibrillin 2 gene haplotype associated with hip dysplasia and incipient osteoarthritis in dogs

Steven G. Friedenberg, MBA, DVM; Lan Zhu, PhD; Zhiwu Zhang, PhD; Wendy van den Berg Foels, PhD; Peter A. Schweitzer, PhD; Wei Wang, BS; Patricia J. Fisher, BS; Nathan L. Dykes, DVM; Elizabeth Corey, BS; Margaret Vernier-Singer, BS; Seung-Woo Jung, DVM, PhD; Xihui Sheng; Linda S. Hunter, DVM, PhD; Sean P. McDonough, DVM; George Lust, PhD; Stuart P. Bliss, DVM, PhD; Ursula Krotscheck, DVM; Teresa M. Gunn, PhD; Rory J. Todhunter, BVSc, PhD

Objective—To determine whether a mutation in the fibrillin 2 gene (*FBN2*) is associated with canine hip dysplasia (CHD) and osteoarthritis in dogs.

Animals—1,551 dogs.

Procedures—Hip conformation was measured radiographically. The *FBN2* was sequenced from genomic DNA of 21 Labrador Retrievers and 2 Greyhounds, and a haplotype in intron 30 of *FBN2* was sequenced in 90 additional Labrador Retrievers and 143 dogs of 6 other breeds. Steady-state values of *FBN2* mRNA and control genes were measured in hip joint tissues of fourteen 8-month-old Labrador Retriever–Greyhound crossbreeds.

Results—The Labrador Retrievers homozygous for a 10-bp deletion haplotype in intron 30 of *FBN2* had significantly worse CHD as measured via higher distraction index and extended-hip joint radiograph score and a lower Norberg angle and dorsolateral subluxation score. Among 143 dogs of 6 other breeds, those homozygous for the same deletion haplotype also had significantly worse radiographic CHD. Among the 14 crossbred dogs, as the dorsolateral subluxation score decreased, the capsular *FBN2* mRNA increased significantly. Those dogs with incipient hip joint osteoarthritis had significantly increased capsular *FBN2* mRNA, compared with those dogs without osteoarthritis. Dogs homozygous for the *FBN2* deletion haplotype had significantly less *FBN2* mRNA in their femoral head articular cartilage.

Conclusion and Clinical Relevance—The *FBN2* deletion haplotype was associated with CHD. Capsular gene expression of *FBN2* was confounded by incipient secondary osteoarthritis in dysplastic hip joints. Genes influencing complex traits in dogs can be identified by genome-wide screening, fine mapping, and candidate gene screening. (*Am J Vet Res* 2011;72:530–540)

Canine hip dysplasia has been the subject of intensive study[1,2] because some large dog breeds have > 50% incidence.[3] The trait has a systemic component because multiple joints can be involved,[4] yet its most conspicuous manifestation is in the hip joint. Debilitating osteoarthritis, which occurs in affected dogs, adversely affects hip function and gait.

Several investigators have explored the origins of hip joint laxity and instability in the supporting structures of the hip joint, especially the hip joint capsule and round ligament of the femoral head, because interruption of such support may be a critical initiating

Abbreviations

CHD	Canine hip dysplasia
DI	Distraction index
DLS	Dorsolateral subluxation
EHR	Extended-hip radiograph
NA	Norberg angle
QTL	Quantitative trait locus
SNP	Single-nucleotide polymorphism

Received October 8, 2009.
Accepted February 16, 2010.
From the Department of Clinical Sciences (Friedenberg, van den Berg Foels, Dykes, Vernier-Singer, Jung, Sheng, Hunter, Bliss, Krotscheck, Todhunter), Microarray Core Facility (Wang), Department of Biomedical Sciences (Fisher, Jung, McDonough, Gunn), and James A. Baker Institute for Animal Health (Corey, Lust), College of Veterinary Medicine, and Institute for Genomic Diversity, College of Agriculture and Life Sciences (Zhang), and Biotechnology Resource Center (Schweitzer), Cornell University, Ithaca, NY 14853; and the Department of Statistics, College of Arts and Sciences, Oklahoma State University, Stillwater, OK 74078 (Zhu).
Supported by Collaborative Research Grant program in the College of Veterinary Medicine, Cornell Biotechnology, the Morris Animal Foundation, the NHLBI Mammalian Genotyping Service, and NIH grant No. 1 R21 AR055228-01A1.
Presented as a poster at the Annual Meeting of the Morris Animal Foundation, Boulder, Colo, June 2007.
The authors thank Alma Jo Williams for technical assistance and Dr. Jody Sandler for contribution of hip joint radiographs and blood samples.
Address correspondence to Dr. Todhunter (rjt2@cornell.edu).

feature of dysplastic hip development.[5] Lust et al,[6] Farese et al,[7] and Smith[8] reported that hip joint laxity, accompanied by synovial effusion and hypertrophy of the round ligament of the femoral head that signal incipient osteoarthritis, contributed to the pathogenesis of CHD.

On the basis of previous genome-wide linkage analysis and fine mapping,[9] we hypothesized that a candidate gene in the QTL interval on CFA11 at 18.5 to 21 cM influenced hip joint laxity, as measured by the DI, in dogs. One gene at 20.3 to 20.5 megabases on CFA11, *FBN2*, was an attractive positional candidate gene because it encodes for a microfibrillary component of extracellular matrix that is present in fibrous joint capsule and articular cartilage.[10] Mutations in *FBN2* are associated with congenital contractural arachnodactyly in humans,[11] and some affected patients have had joint laxity. The purpose of the study reported here was to determine whether a mutation in *FBN2* is associated with CHD and osteoarthritis in dogs.

Materials and Methods

Cornell DNA Hip Archive—Study dogs were from closed breeding colonies at the Baker Institute for Animal Health at Cornell University and Guiding Eyes for the Blind (Yorktown Heights, NY), and dogs admitted to the Cornell University Hospital for Animals. There was DNA available from 210 Labrador Retrievers bred from 1989 over 8 generations. More recently, the authors developed a crossbreed pedigree for QTL mapping of CHD founded with 7 unaffected Greyhounds (2 males and 5 females) and 8 Labrador Retrievers (4 males and 4 females) with CHD and secondary osteoarthritis.[12] The pelves of dogs from the Baker Institute for Animal Health underwent radiography between 8 and 12 months of age, whereas the dogs from Guiding Eyes for the Blind underwent radiography between 14 and 18 months of age. The pedigrees of all available dogs were used to derive breeding values for hip trait mapping. The final data set contained Labrador Retrievers, Greyhounds, their crossbred offspring, and 14 other breeds, totaling 1,551 dogs that had at least 1 of the 4 radiographic hip measurements. Ancestry of these 1,551 dogs was traced back as far as 17 generations, resulting in a total of 2,716 dogs, including 1,498 dogs from Guiding Eyes for the Blind, 571 from the Baker Institute for Animal Health, 425 from the Cornell University Hospital for Animals, and 222 ancestors traced from the Orthopedic Foundation for Animals semiopen database.[13] The study was approved by the Cornell University Institutional Animal Care and Use Committee.

Phenotyping—The severity of CHD was measured from pelvic radiographs by use of the NA,[14] DI,[15,16] DLS score,[17] and EHR projection score adopted by the Orthopedic Foundation for Animals and by evaluation of hip osteoarthritis (new bone formation on the femoral head and neck and acetabular osteophytes) on the EHR. Although these radiographic measurements were correlated,[18] none of the measurements completely replaced the other so that at least 2 of them are required to represent a dysplastic hip joint.

Narrowing the QTL interval on CFA11—A QTL for CHD on 12 chromosomes in a Greyhound–Labrador Retriever pedigree was previously identified.[19] To improve genome coverage, these dogs were later genotyped at 225 additional microsatellites of minimal screening set 2 on 16 chromosomes.[20–22] Linkage analysis confirmed the presence of a QTL for CHD segregating in the crossbreed pedigree with a maximum logarithm of odds peak score of 3.45 on CFA11 at 36 cM for the second principal component of the DLS score and DI. Genotyping was performed on 257 dogs, including Labrador Retrievers, Greyhounds, and their crossbred offspring, at 111 SNPs in this QTL region on CFA11. Multipoint linkage analysis[23] revealed substantial evidence for 2 QTLs contributing to the DI between 15.7 to 17 cM and 18.5 to 21 cM (95% posterior probability interval), which explained approximately 15% to 18% of the total variance in the DI.[9] *FBN2*, a candidate gene at 20.3 to 20.5 megabases, was within this interval.

***FBN2* screening**—The exon structure of *FBN2* was identified by use of an online genome browser[a] and National Center for Biotechnology Information[b] and University of California-Santa Cruz[c] genome databases of the second release of the *Canis familiaris* genome sequence. Primer sequences were designed by use of software[24] and ordered from a commercial source[d] and are available from the primary author (SGF). Exons were amplified from genomic DNA via PCR under standard conditions. Amplicons were purified.[e,f] Each exon was sequenced initially in the forward direction only, then in the reverse direction if necessary. Sequencing was performed on a commercial sequencer.[g] In addition, introns 1 and 2 and 372 bp upstream of exon 1 were sequenced from genomic DNA to identify regulatory regions that might affect gene expression. Sequence was analyzed by use of commercial software.[h]

Sequencing and association study—*FBN2* was first sequenced in 21 Labrador Retrievers and 2 Greyhounds. Intron 30 of *FBN2* was then sequenced in a larger number of dogs selected from the dogs in the CHD DNA archive. Dogs were chosen by use of an algorithm to maximize genetic diversity and minimize relatedness.[25] Dog selection based on phenotype was performed by use of the principal components of the DI, DLS score, EHR score, and NA, weighted by their eigenvalues. Intron 30 of *FBN2* was sequenced in 90 additional Labrador Retrievers, 18 Border Collies, 47 German Shepherd Dogs, 29 Golden Retrievers, 29 Newfoundlands, 19 Rottweilers, and 1 Great Dane. The PCR primers (forward, 5′–ggccaatgtaccaacattcc; reverse, 5′–tgaaggatcccttggtgttc) were designed to amplify intron 30 of *FBN2* and included at least 50 bp in either direction by use of commercial software.[24] M13 universal primers were added to the 5′ end of each primer to facilitate sequencing.

Characterization of *FBN2* expression—Specimens of the dorsal fibrous joint capsule, round ligament of the femoral head, and full-thickness noncalcified articular cartilage from the dorsal surface of the femoral head but not including the perifoveal area were collected from fourteen 8-month-old Labrador Retriever–Greyhound crossbred dogs at necropsy. Six of the dogs were from one litter (three-quarter Labrador Retriever and one-quarter Greyhound [litter 1]), and the remaining 8 dogs were from another litter (seven-eighth Labrador

Retriever and one-eighth Greyhound [litter 2]).[12,19] The joints were evaluated grossly for evidence of osteoarthritis as the traditional indication of hip dysplasia.[17]

Tissue was harvested within 2 hours of euthanasia. Samples from the right hip joint of each dog were used for mRNA isolation. Samples from litter 1 were flash frozen in liquid nitrogen and stored at –80°C, and samples from litter 2 were preserved for later RNA extraction[i] and stored at –20°C. The RNA was isolated by use of a commercial kit designed to extract RNA from fibrous tissues.[26] Briefly, approximately 150 mg of each frozen sample was placed in a stabilizing buffer and homogenized 2 or 3 times for 30 to 45 seconds on ice. The homogenate was incubated at 55°C for 20 minutes with proteinase K and was then pelleted by centrifugation at 4,500 × *g* to remove cellular debris. The supernatant solution was collected, a 0.5 volume of 100% ethanol was added, and the solution was filtered via centrifugation at 4,500 × *g* through a silica column designed to bind RNA. DNAse I was added to the bound RNA to remove any contaminating DNA. The sample was washed and eluted in nuclease-free water. Concentrations and purity were assessed spectrophotometrically.

Expression of *FBN2* was measured via quantitative reverse transcription PCR assay. First, cDNA was prepared from each RNA sample. One microgram of RNA was added to a standard mixture of deoxynucleotide triphosphates (4×), random primers (1×), recombinant Moloney murine leukemia virus reverse transcriptase (1×), and reaction buffer (1×) in a 1:1 (vol/vol) RNA:mixture ratio. Reactions were incubated in a thermal cycler, annealment was performed at 25°C for 10 minutes, copying was performed at 37°C for 2 hours, and inactivation was performed at 85°C for 5 seconds. Custom primers and probes were designed to amplify portions of *FBN2* cDNA at the junctions of exons 4-5, 30-31, and 59-60 (**Appendix 1**). Glucose phosphate isomerase was used as an endogenous control with a single probe at the exon 2-3 junction. Probes were labeled with 6-carboxy-fluorescein and a nonfluorescent quencher and synthesized by the manufacturer[g] at a 20× concentration. Second-step reactions were prepared as follows: approximately 60 ng of cDNA, each primer-probe mix (1×), and commercial master mix (1×)[g] in a final volume of 20 µL. Each PCR reaction was carried out in quadruplicate[g] and activated at 95°C for 10 minutes, followed by 40 repeat cycles of 15-second denaturation at 95°C, followed by annealing-extension at 60°C for 1 minute. Relative quantification was performed by use of the mean difference in threshold cycle values of all the samples for a particular probe as the calibrator; difference in threshold cycle values were read midway into the linear phase of the amplification curve. Expression of control genes *FBN1*, kinesin 11 (*KIN11*), and topoisomerase 1 (*TOP1*) was similarly measured.[g]

Alternative splicing—Two or 3 mRNA samples isolated from fibrous joint capsule, round ligament, and articular cartilage from dogs of each intron 30 *FBN2* genotype (unaffected homozygous, heterozygous, and affected or deletion homozygous) were selected for further analysis. One-step reverse transcription PCR amplification of these samples was performed in regions adjacent to intron 30 in 2 experiments. In the first experiment, 1 upstream primer was selected within exon 26 and downstream primers were chosen within exons 28, 29, 30, 31, and 33 (**Appendix 2**). In the second experiment, 1 upstream primer was chosen within exon 34 and downstream primers were chosen within exons 36, 37, 39, 40, 41, 42, and 43. The reverse transcription PCR amplification was performed by use of a 1-step reverse transcription PCR system.[j] Briefly, 250 ng of template RNA was mixed with 2 U of reverse transcriptase and 0.2 µM of each primer and reaction buffer and incubated. Thermal cycler temperatures were 55°C for 30 minutes, 94°C for 2 minutes, 40 cycles of 94°C for 15 seconds, 55°C for 30 seconds, 68°C for 1 minute, and 68°C for 5 minutes. The PCR reaction products were analyzed on a 2% agarose gel to detect amplicons shorter than expected.

Immunohistochemical analyses—Formalin-fixed sections of dorsal hip capsule from affected and unaffected crossbred dogs from which the mRNA was isolated and amplified were also examined by use of H&E stain; Vierhoff von Giesen stain for elastin fibers was also used. The elastin stain revealed sparse numbers of short fibrils concentrated primarily beneath the synovial lining in the loosely arranged connective tissue. For immunohistochemical analyses, sections were deparaffinized, blocked with 0.5% H_2O_2 in methanol, and washed with distilled H_2O and Tris-buffered saline solution[k] (pH 7.6). Sections were blocked with 10% normal goat serum with 2× casein[l] for 20 minutes, and incubated for 2 hours at 37°C with rabbit anti-*FBN2*[m] monoclonal antibody diluted 1:40 in Tris-buffered saline solution with 1× casein. After washing with Tris-buffered saline solution, biotinylated goat anti-rabbit IgG[n] was applied at 1:200 for 20 minutes at 20°C, followed by Tris-buffered saline solution washes and incubation for 20 minutes with streptavidin peroxidase.[l] The substrate was prepared as directed[l] and applied for 10 minutes. Slides were counterstained with hematoxylin and mounted.[o] Controls were included, substituting normal rabbit IgG[k] in place of primary antibody. Immunohistochemical staining for *FBN2* expression was compared with serial sections treated with normal rabbit serum. The intensity of staining was subjectively graded.

Statistical analysis—The effect of the *FBN2* haplotype on each hip joint measurement was evaluated in cumulative distribution plots. The cumulative distribution plots were compared with results of the Kolmogorov-Smirnov test. The linear model used to test the effect of the *FBN2* haplotype on hip dysplasia was as follows:

Radiographic trait = Mean for the trait + sex + breed (Labrador Retriever or non–Labrador Retriever) + body weight + age + *FBN2* haplotype + interactions

where the interaction term included all possible pairwise interactions. Variable selection strategy was performed to find the final linear model with significant ($P < 0.05$) terms only. This model was applied to each of the 4 CHD traits. Given any randomly sampled dog of known breed and body weight and knowing its *FBN2*

haplotype, a prediction interval for the hip trait was calculated.

Values for expression of mRNA were log transformed and tested as a function of the presence or absence of secondary osteoarthritis or CHD phenotypes (DLS score, NA, and EHR score) in a mixed linear model that included the covariates of the dog's genotype at the *FBN2* locus, sex, age, and body weight, with a random effect for litter. To test the effect of hip joint phenotype on the expression of the control genes, *FBN1*, *TOP1*, and *KIN11* in fibrous joint capsule, the *FBN2* genotype was not included in the model. The effect of the hip joint phenotype on the expression of *FBN1* and *FBN2* only was tested in the femoral head articular cartilage. For all comparisons, values of $P < 0.05$ were considered significant.

Results

Dogs and phenotypes—Twenty-three dogs were first selected for *FBN2* sequencing of genomic DNA. One group of 12 affected Labrador Retrievers had EHR scores ≥ 5, NAs < 100°, and DLS scores < 45° for both hip joints. The other group of 11 unaffected dogs included 9 Labrador Retrievers and 2 Greyhounds with EHR scores ≤ 2, NAs > 107°, and DLS scores > 55° in both hip joints. The hip joint phenotypes of an additional 90 Labrador Retrievers and 143 non–Labrador Retrievers used to sequence intron 30 of *FBN2* were determined (**Figure 1**). Of the 257 dogs originally used in SNP fine mapping that localized the QTL to 18 to 21 cM on *CFA11*,[14] only 8 Labrador Retrievers from the Baker Institute for Animal Health and 11 German Shepherd Dogs satisfied the criteria for *FBN2* sequencing of genetic and phenotypic diversity. Of the 14 Labrador Retriever crossbred dogs used for quantitative reverse transcription PCR analysis of *FBN2*, *FBN1*, *TOP1*, and *KIN11*, 6 dogs had early hip joint osteoarthritis at necropsy characterized by perifoveal articular cartilage fibrillation, and 8 dogs had no gross signs of hip joint osteoarthritis. Only 1 dog had unilateral (right) hip joint osteoarthritis and no signs of osteoarthritis in the opposite hip joint. For these dogs, mean ± SD right hip joint DLS score was 48 ± 6.3 (range, 41% to 62%), mean ± SD EHR score was 2.4 ± 1.2 (range, 1 to 5), and mean ± SD NA was 99.3 ± 5 (range, 90° to 105°).

Sequencing—A haplotype was identified within the first 100 bp of intron 30 in *FBN2* that segregated in 12 Labrador Retrievers affected with CHD (AGC haplotype) and 9 Labrador Retrievers and 2 Greyhounds unaffected with CHD (GAT haplotype; **Appendix 3**). The GAT haplotype extended downstream (TACTTTA between bp 189 and 195 where the 7-bp deletion for the AGC haplotype occurred) within intron 30. Additional sequencing revealed that the GATTACTTTA haplotype in intron 30 extended further downstream, with A at intron 37 base 27, C at intron 40 base 32, and T at exon 41 base 143; the latter caused no change in amino acid sequence. In these same positions, the haplotype continued downstream as follows: G-A-C for the AGC (deletion) haplotype, and R-M-Y for the heterozygous haplotype. Via sequencing of 372 bp upstream of *FBN2* exon 1, an SNP was found that was not associated with the 2 groups that were either affected or unaffected with CHD. It was not possible to sequence farther upstream. In the same group of dogs, intron 2 was also sequenced and none of the 3 SNPs discovered was associated with CHD in the same dogs.

The DNA from an additional 90 Labrador Retrievers and 143 non–Labrador Retrievers was sequenced for the same *FBN2* haplotype in intron 30. The cumulative trait distributions for the effect of the 3 genotypes on each hip joint trait on the Labrador Retrievers were determined (**Figure 2**). The cumulative distribution plots of the Labrador Retrievers homozygous for the AGC haplotype were significantly different, compared with either of the other 2 haplotypes for all traits except the left NA ($P = 0.08$), the right DI ($P = 0.08$), and both left and right EHR scores (largest $P = 0.29$). However, via analysis in a linear model with covariates, dogs homozygous for the AGC (deletion) haplotype had worse hip joint conformation characterized by a lower DLS score, higher DI, lower NA, and higher EHR score than did those with the GAT or heterozygous haplotype (**Figure 3**).

An example of the effect of the *FBN2* genotype on a CHD trait (the ANOVA table for the effect of haplotype, body weight, and breed on the left NA) was developed (**Table 1**). Other hip joint traits were similarly affected

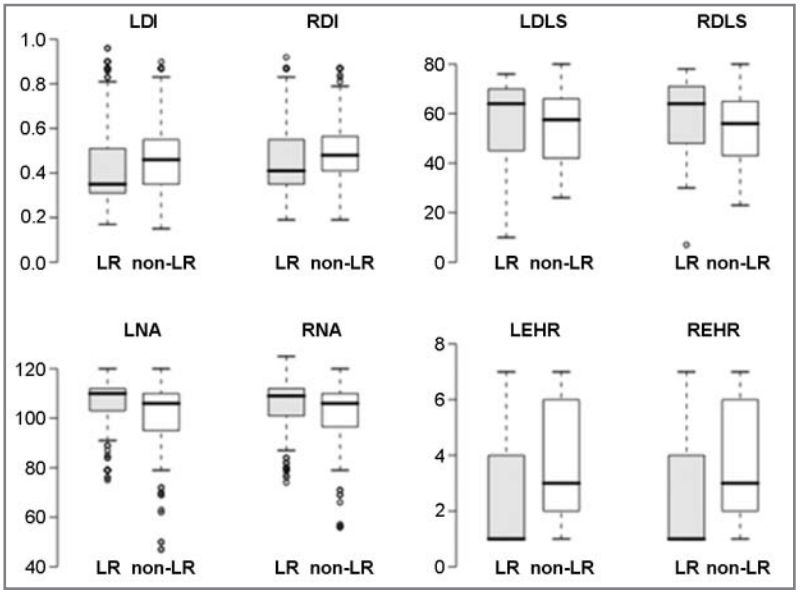

Figure 1—Box-and-whiskers plots of hip joint radiographic phenotypes of 90 Labrador Retrievers (LR) and 143 non–Labrador Retrievers (non-LR) used for sequencing of intron 30 of *FBN2*. LDI = Left DI. LDLS = Left DLS score. LEHR = Left extended hip joint radiographic score. LNA = Left NA (degrees). RDI = Right DI. RDLS = Right DLS score. REHR = Right extended hip joint radiographic score. RNA = Right NA (degrees). The y-axes are the span of measurements for that trait in the dogs tested. The dark horizontal line indicates the median, and the box indicates the interquartile range. The highest and lowest values are indicated by the horizontal lines at the ends of the vertical dotted lines; circles indicate outliers.

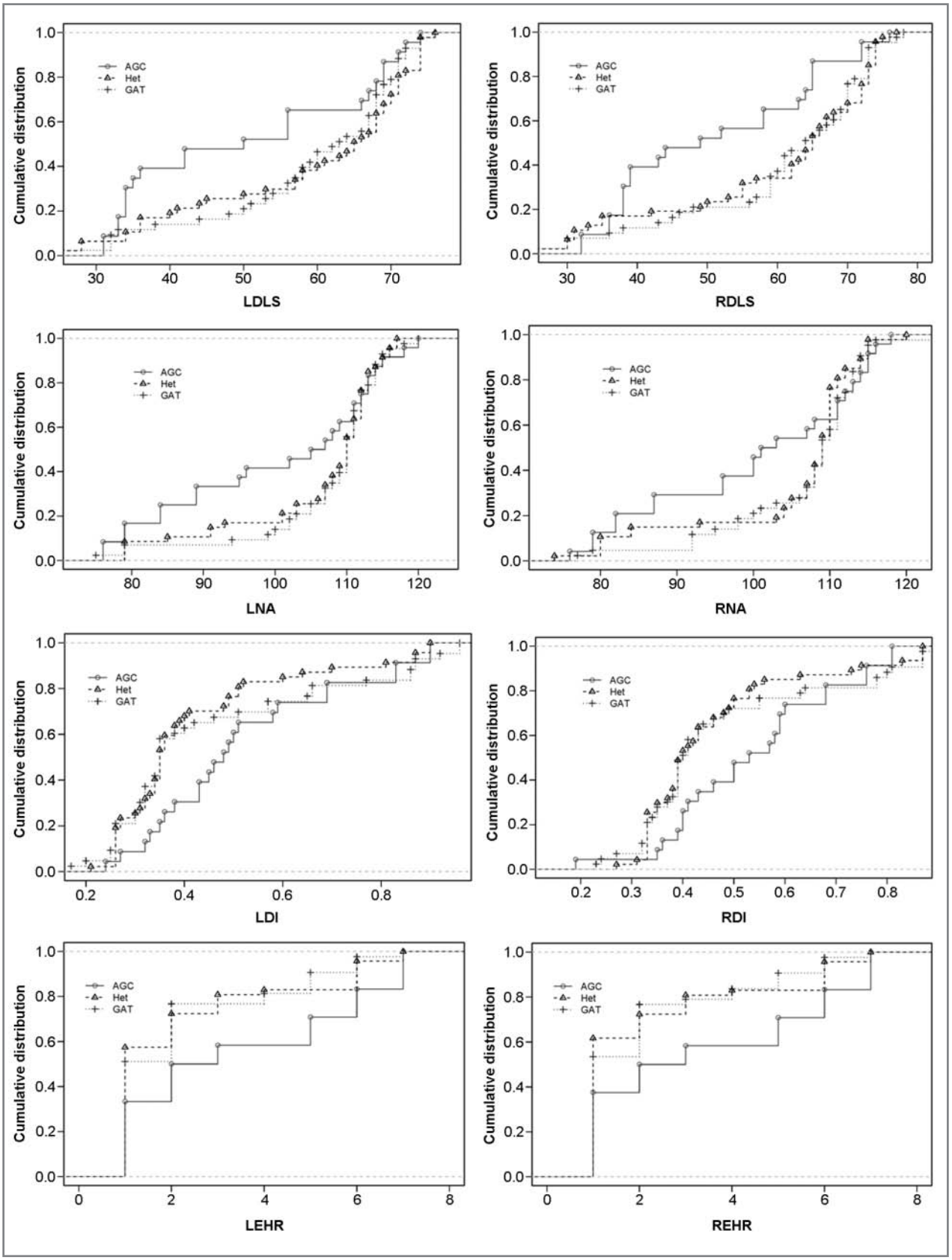

Figure 2—Cumulative distribution (proportion) plots for Labrador Retrievers genotyped for the *FBN2* haplotype illustrating the cumulative effect of the *FBN2* haplotype on each dog's hip joint measurement (the left [L] and right [R] DLS score [n = 101 dogs], NA [102], DI [101], and EHR score [102]). AGC indicates homozygosity for the *FBN2* deletion. GAT indicates homozygosity for the unaffected haplotype. Het = Heterozygote. *See* Figure 1 for remainder of key.

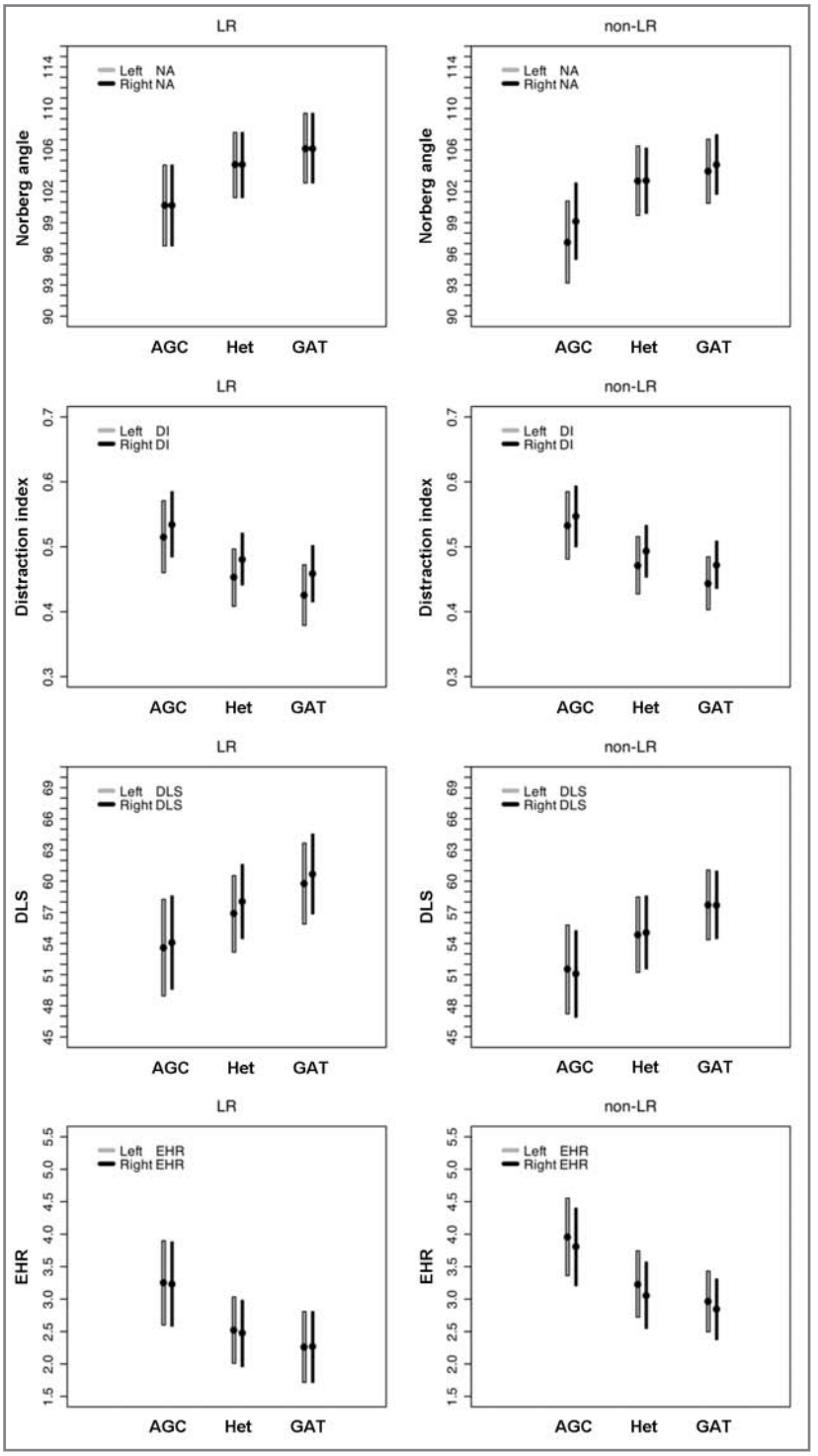

Figure 3—Plots of the effect of *FBN2* intron 30 haplotype on the left and right hip joint measurements for 110 Labrador Retrievers (DI and DLS data from 109 dogs) and 132 non–Labrador Retrievers. Points represent the means and bars represent the 95% confidence intervals for each of the 3 haplotypes. *See* Figures 1 and 2 for remainder of key.

by the haplotype. Because the dog's sex, age when the radiograph was taken, and all other interaction terms except body weight by breed were not significant, these variables were dropped from the model. This linear model explained approximately 14% of the total variation in the left NA.

For any randomly sampled Labrador Retriever with body weight of 30 kg that was homozygous for the deletion AGC haplotype, the equation for the estimated left NA was as follows:

$$LNA_{LR,AGC,weight} = 76.15 + 0.79 \bullet body\ weight = 76.15 + 0.79 \bullet 30 = 99.9°$$

where LR is Labrador Retriever breed. For a similar dog homozygous for the GAT haplotype, the equation for the estimated left NA was as follows:

$$LNA_{LR,GAT,weight} = 76.15 + 6.84 + 0.79 \bullet body\ weight = 106.7°$$

For a similar but heterozygous Labrador Retriever, the equation for the estimated left NA was as follows:

$$LNA_{LR,het,weight} = 76.15 + 5.91 + 0.79 \bullet body\ weight = 76.15 + 5.91 + 0.79 \bullet 30 = 105.8°$$

where het is heterozygous. However, the interaction of breed and body weight contributed significantly to the variation of the NA. Heavy Labrador Retrievers had higher NAs than did heavy non–Labrador Retrievers. Similar interactions of body weight occurred with the other hip joint traits (data not shown).

***FBN1*, *FBN2*, *KIN11*, and *TOP1* expression and immunohistochemical analysis**—In the mixed linear model, the effects of sex, age, and body weight on gene expression were not significant and these terms were dropped from the model. As the DLS score decreased by 1%, *FBN2* expression in the fibrous joint capsule increased by approximately 5% (**Tables 2–5**). The model including the DLS score and hip joint osteoarthritis explained approximately 40% of *FBN2* expression. Dogs that had incipient osteoarthritis at necropsy as the traditional indicator of prior CHD had approximately 50% greater *FBN2* mRNA in their hip joint capsule than did dogs with nonaffected hip joints. Dogs with the AGC homozygous genotype had less *FBN2* expression in hip joint capsules, although the difference was not significant. In the femoral head articular cartilage, the GAT homozygous dogs had significantly higher *FBN2* expression, compared with the heterozygotes and dogs homozygous for the AGC (deletion) haplotype. There was no evidence of alternatively spliced *FBN2* transcripts resulting from the deletion in intron 30 in mRNA transcript isolated from the joint capsule.

Most immunostaining for *FBN2* was seen in the subsynovial region of the hip joint capsule (**Figure 4**). No qualitative difference was observed in immunostaining of *FBN2* in the hip joint capsule of affected hip joints, compared with unaffected hip joints.

There was no significant difference in mRNA expression in the fibrous joint capsule of *FBN1* and *TOP1* of dogs with osteoarthritis, compared with those without osteoarthritis. However, *KIN11* mRNA expression was significantly greater in the joint capsules of osteoarthritic hip joints (Tables 2–5). For each unit increase (worsening) of the EHR score, the *KIN11* expression increased by 34%. There was no effect of litter or tissue preparation on gene expression.

Table 1—Estimated coefficients for the effects of the *FBN2* haplotype, body weight, and breed on the left NA in dogs.

Coefficient	Estimate	SE	*P* value
Intercept	76.15	9.50	6.72
Haplotype GAT	6.84	2.29	0.003
Haplotype het	5.90	2.31	0.01
Body weight	0.79	0.29	0.001
NLR breed	31.73	10.13	0.001
NLR breed body weight	–1.15	0.31	< 0.001

Each genotype and osteoarthritis class of the fixed-effect variables is compared with the class with the lowest estimate.
het = Heterozygote. NLR = Non–Labrador Retriever.
Multiple R^2 = 0.143; adjusted R^2 = 0.124.

Table 2—Results of ANOVA for *FBN2* expression in the fibrous joint capsule of 14 Labrador Retriever–Greyhound crossbred dogs with and without hip joint dysplasia as a function of the presence (aff) or absence of osteoarthritis after adjusting for each dog's genotype at intron 30 of *FBN2*.

Coefficient	Estimate	SE	*P* value
Intercept	–0.16	0.41	0.76
Genotype aff	–0.02	0.28	0.49
Genotype het	0.04	0.18	0.83
Osteoarthritis aff	0.52	0.22	0.03

aff = AGC homozygote.
See Table 1 for remainder of key.

Table 3—Results of ANOVA for *FBN2* expression in the fibrous joint capsule of 14 Labrador Retriever–Greyhound crossbred dogs with and without hip joint dysplasia as a function of the DLS score after adjusting for each dog's genotype at intron 30 of *FBN2*.

Coefficient	Estimate	SE	*P* value
Intercept	1.94	0.93	0.28
Genotype aff	0.59	0.33	0.10
Genotype het	0.52	0.26	0.06
DLS score	–0.05	0.02	0.03

See Tables 1 and 2 for key.

Table 4—Results of ANOVA for *KIN11* expression in the fibrous joint capsule of 14 Labrador Retriever–Greyhound crossbred dogs with and without hip joint dysplasia as a function of the EHR score after adjusting for each dog's genotype at intron 30 *FBN2*.

Coefficient	Estimate	SE	*P* value
Intercept	–0.49	0.31	0.36
Genotype aff	–0.48	0.26	0.11
Genotype het	–0.07	0.20	0.71
EHR score	0.34	0.13	0.04

See Tables 1 and 2 for key.

Discussion

The candidate gene, *FBN2*, was identified through genome-wide, microsatellite-based screening of a Labrador Retriever–Greyhound pedigree, followed by narrowing of the QTL region on *CFA11* through multipoint linkage analysis with SNP genotypes. An association between a mutation-deletion haplotype in *FBN2* and CHD was detected. This is the first gene reported to be associated with all 4 CHD radiographic measurements, an important orthopedic trait that leads to debilitating hip joint osteoarthritis. The *FBN2* mutation was identified in an initial set of 23 dogs and in additional Labrador Retrievers and dogs of other breeds. Only 19 of the 257 dogs in which the QTL for the DI was originally identified[14] were later subjected to *FBN2* sequencing. The authors made the a priori decision not to include crossbred dogs from our colony in the analysis. We reasoned that testing the mutation in unrelated purebred dogs, most of which were not included in prior linkage analyses, would strengthen support for any association discovered. In hindsight, it is probably wise to screen for segregation of a candidate gene mutation in the subset of the individuals originally used in the linkage study prior to validation of a mutation discovery in a new population. The AGC allele had recessive characteristics because the heterozygous and homozygous GAT individuals were similar phenotypically. Clearly, other genes must contribute to CHD because the *FBN2* locus does not explain all the genetic trait variation in CHD. This is consistent with the results of QTL mapping in Labrador Retriever–Greyhound crossbred dogs,[19] Labrador Retrievers,[22] German Shepherd Dogs,[2] and Portuguese Water Dogs,[27] in which no locus for CHD was identified that contributed > 18% of trait variance.

Expression of *FBN2* in the joint capsule was related inversely with the DLS score; that is, as the right DLS score decreased (a worse hip joint conformation), the *FBN2* expression increased in the right hip joint capsule. It was expected that *FBN2* expression would be lower in dogs with lower DLS scores because the dogs that were homozygous for the deletion (AGC) haplotype had significantly lower *FBN2* expression in their femoral head articular cartilage. One explanation is that the experiments were confounded by the presence of secondary osteoarthritis in dysplastic hip joints. The

Table 5—Results of ANOVA for *FBN2* expression in the femoral head articular cartilage of 14 Labrador Retriever–Greyhound crossbred dogs with and without hip joint dysplasia as a function of the presence or absence of osteoarthritis after adjusting for each dog's genotype at intron 30 of *FBN2*.

Coefficient	Estimate	SE	*P* value
Intercept	0.43	1.34	0.02
Genotype unaff	10.35	2.12	0.01
Genotype het	1.69	1.70	0.35
Osteoarthritis unaff	0.80	1.85	0.73

unaff = GAT homozygote. *See* Tables 1 and 2 for remainder of key.

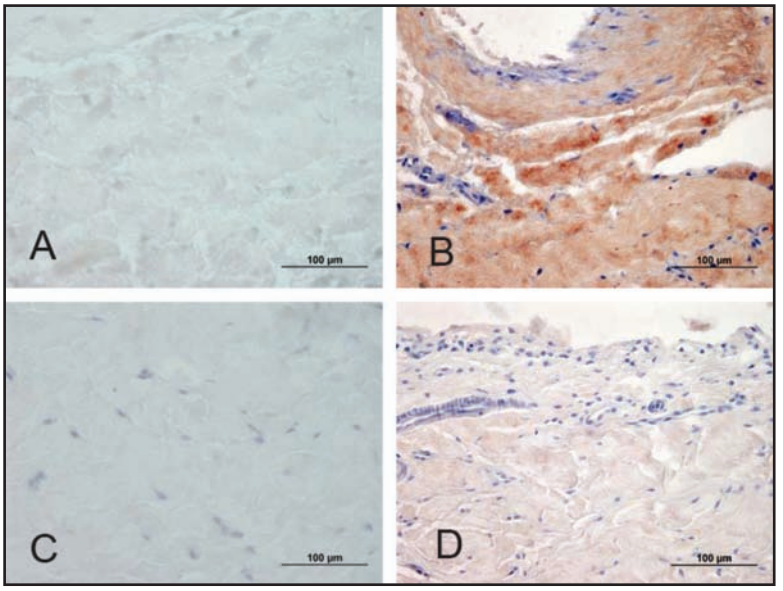

Figure 4—Photomicrographic views of hip joint capsule specimens from dogs. A—Histologic section of a hip joint capsule specimen from a dog without osteoarthritis (immunohistochemical stain; negative control [IgG]). B—Same section as in panel A, stained with anti-*FBN2* antibody. Notice the moderately intense diffuse immunostaining (brown-red) of the subsynovial collagenous matrix. C—Histologic section of a joint capsule specimen from a dog with hip joint osteoarthritis. The synovial lining is at the top of the image (immunohistochemical stain; negative control [IgG]). D—Same section as in panel C, stained with anti-*FBN2* antibody. Notice that immunostaining of the tissue is low, compared with that in panel B.

presence of osteoarthritis was used as the definitive criterion for a dysplastic hip joint. The perifoveal area is the location where the incipient gross alterations in femoral head articular cartilage are observed. This tissue was deliberately excluded from analysis. The expression of the genes studied may not change as rapidly with incipient osteoarthritis in the chondrocytes in dorsal articular cartilage as in the fibroblasts in joint capsules.

FBN2 mRNA expression was examined in the hip joint tissues of the dogs when they reached approximate skeletal maturity (8 months of age). It is not known whether *FBN2* is differentially expressed during canine joint development. In mice, *FBN2* expression occurs early in development in the perichondrium, periosteum, and acetabulum; however, the joint capsule and round ligament were not included in that analysis.[28] In mice, *FBN1*expression occurs later in development but its expression remains high. Most of the tissue alterations that result in a dysplastic hip joint occur during the period of rapid growth, which for a large-breed dog like a Labrador Retriever slows at approximately 6 months of age, and more rapidly growing dogs develop a more severe form of CHD.[29,30] Therefore, examination of *FBN2* expression during the growth period is warranted. This would require biopsy of hip joint tissues of growing dogs of differing susceptibility to CHD and with known *FBN2* genotype, then confirming the diagnosis at maturity. Finally, mRNA concentrations from a gene and the concentration of the expressed protein are not always strongly correlated.[31,32] Protein studies may be required to reach any firm conclusions about the role of *FBN2* in hip joint development and CHD. The analysis of tissues from only 14 dogs and the crossbreed genetic background of these dogs, which contained up to one-quarter Greyhound genes, could have influenced the results.

The fibrillins belong to a family of structurally related glycoproteins that include the latent transforming growth factor-β–binding proteins and fibulins.[10] Fibrillins are the major structural components of extracellular microfibrils, which are either associated with elastin or act as elastin-free assemblies.[33] Mutations in the gene encoding *FBN2* have been associated with human congenital contractural arachnodactyly, a disorder characterized by arachnodactyly (elongated distal long bones), dolichosternomelia (elongated limbs), scoliosis, multiple congenital contractures, and abnormalities of the external portion of the ears.[30] A similar phenotype was produced in mice through a deletion of the *FBN2* gene.[34] Most of the mutations discovered in *FBN1* and *FBN2* occur in the same region (ie, upstream or downstream of exon 30) as for the mutation discovered in dogs with CHD in the present study. The CHD phenotype is genetically complex, and the effect of any *FBN2* haplotype would not be expected to be as severe as the *FBN2* knockout phenotype in the mouse. The joint contractures in humans with congenital contractural arachnodactyly disappear with aging.[10] Mice heterozygous for the *FBN2* mutation do not have an abnormal phenotype unless they are also heterozygous for a mutation in bone morphogenetic protein 7.[35] Some human patients with congenital contractural arachnodactyly have joint laxity including hypermobile thumbs.[11] However, the mechanism by which such an intron deletion in *FBN2* may contribute to the CHD phenotype remains unclear.

Fibrillins are present in the chondroepiphysis of the developing joint.[36,37] Because congenital contractural arachnodactyly is characterized by deformation of the pinnae, Yanagino et al[38] examined the regulation of *FBN2* in chondrocytic differentiation of murine ATDC5 cells. The *FBN2* was highly expressed in the early stage of differentiation and later declined. The 5′ flanking region of *FBN2* contains potential binding sites for the E2 factor (F1) family, Runx, AP-2, and Sox transcription factors. Overexpression of *E2F1* results in a marked increase in *FBN2* promoter activity. Because the dogs homozygous for the *FBN2* deletion mutation had lower *FBN2* expression in femoral head cartilage, examination of *FBN2* expression in chondroepiphyseal cartilage of the developing hip joint might further elucidate the functional importance of the *FBN2* mutation. However, biopsy of femoral chondroepiphyseal tissue during development would damage the hip joint and result in osteoarthritis.

The mechanism by which altered concentrations of FBN2 protein might interrupt the mechanical integrity of the hip joint capsule or femoral head articular cartilage contributing to hip joint laxity and dysplasia

remains unknown. Even small changes in gene expression may influence complex behavioral traits, such as geotaxis in *Drosophila* spp.[39] The compliance of the joint capsule and round ligament of the femoral head relies partly on its elastic tissue content and distribution, and fibrillins are a component of the elastic tissue. In the fibrous hip joint capsule of monkeys, elastic tissue predominates caudodorsally and ventrally, compared with craniodorsally.[40] So-called ball and socket joints such as the hip joint and shoulder joint require pliable and extensible capsular support devoid of strong collateral ligaments. Electron microscopic images of the hip joint capsule of an 8-month-old Labrador Retriever with a lax (high DI) joint capsule revealed that the cross-sectional diameter of the collagen fibrils was heterogeneous.[41] The cross-sectional collagen fibrillar diameter in the hip joint capsule of a Labrador Retriever without CHD and with tight hip joints was uniform. Flexor digitorum longus tendons from mice null for *FBN2* have the same collagen content as control mice but contain fewer intermolecular collagen cross-links of hydroxylysyl and lysyl pyridinoline.[36] The collagen of femoral heads of dysplastic Labrador Retrievers is more soluble than the collagen of femoral heads of unaffected puppies. Electron micrographs of articular cartilage of the same femoral heads reveal disruption of collagen fibrils in young dogs with CHD.[42–44] The etiology of this disruption, which was discovered through an electron microscopic and biochemical evaluation decades ago, has never been elucidated, but a plausible explanation may now be possible to achieve through positional cloning of contributing genes.

Understanding the genetic basis of CHD will help identify similar biochemical pathways that lead to developmental dysplasia of the human hip joint, for which there also is evidence of a genetic basis. Previous studies[45,46] that examined the underlying biochemical mechanism for hip joint laxity in humans examined the capsular collagens. Increased collagen type III-to-type I ratios in hip joint capsules of dysplastic human neonates have been reported.[46,47] Similar findings of increased ratios of type III to type I collagen propeptides in synovial fluid have been reported in the hip joints of dysplastic dogs, compared with unaffected dogs.[48] The action of the maternal hormones estrogen, relaxin, and testosterone on genetically susceptible hip joint tissues may contribute to hip joint laxity in the perinatal period,[49] but whether this effect persists is unknown. Fibrillin 2 is the preferred target for relaxin activity and expression, compared with fibrillin 1, as measured in human dermal fibroblasts and murine fetal skin.[50] Because extracellular matrix proteins, such as the fibrillins, sequester TGF-β–signaling molecules, the effect of fibrillin concentration may be indirect. The location of TGF-β molecules affects the function of surrounding cells and the entire extracellular matrix.[10] Impaired microfibril assembly can result in excess local TGF-β signaling,[10] which participates in the pathogenesis of ruptured aortic aneurysm in Marfan syndrome, a result of an *FBN1* or TGF-β signaling mutation.

Other genes in linkage disequilibrium with *FBN2* may contribute to the QTL on *CFA11* at 18.5 to 21 cM. We excluded a chondroitin sulfate synthase gene (*CSS3*) and a disintegrin and metalloproteinase with thrombospondin motifs gene (*ADAMTS19*, a member of the aggrecanase family in this interval) as candidates for CHD via direct sequencing in affected and unaffected Labrador Retrievers and found no mutations. Another gene warranting sequencing in the interval includes solute carrier family 12 member 2, a gene associated with loin muscle mass in pigs. Greyhounds, a breed resistant to CHD, have higher muscle-to-bone mass ratios than do Labrador Retrievers, possibly implicating the loin muscle mass gene in the pathogenesis of CHD.[51]

Dysplastic hip joints as measured by the DLS score and osteoarthritis had significantly higher *FBN2* expression in hip joint capsules, compared with unaffected joints. The *KIN11* expression was also increased in the joints with osteoarthritis, compared with expression in the unaffected joints, but expression of *TOP1* and *FBN1* was unaffected. The most dysplastic joints were in the incipient stages of osteoarthritis with perifoveal articular cartilage fibrillation and synovitis. Gene expression is globally increased in the early stages of canine osteoarthritis,[52] so it was not surprising that at least one of the genes chosen as a control gene had high mRNA expression in joints with osteoarthritis. KIN11 protein is a major component of intracellular machinery.[53] Gross evidence of osteoarthritis was chosen in the present study as the traditional indicator of concomitant CHD because there is no precisely accurate method to assess functional or dynamic subluxation of a dysplastic hip joint that results in osteoarthritis. The DLS score alone has approximately 80% accuracy for predicting osteoarthritis of the hip joint as measured via combined sensitivity and specificity.[18] All the radiographic methods of hip joint assessment are performed with the dog passively positioned and recumbent, and radiographs do not reveal the incipient stages of osteoarthritis in the hip joint. Besides those genes that influence the expression of CHD, other genes likely influence the onset and progression of hip joint osteoarthritis in dysplastic hip joints.

The mapping and identification of *FBN2* as the first gene reported to be associated with CHD indicate that complex traits such as CHD can be evaluated in dogs at the molecular genetic level. The strategy of coarse genome screening with microsatellites or SNPs followed by fine mapping with SNPs can resolve a QTL to a small interval suitable for candidate gene screening.[54] The association between the *FBN2* deletion haplotype and CHD was detected in Labrador Retrievers and non–Labrador Retriever breeds, indicating that some of the genes that contributed to CHD were conserved across breeds. Further studies are needed to elucidate the biochemical pathway through which mutations in *FBN2* might influence in the developmental pathogenesis of CHD.

a. Ensembl [database online]. Cambridge, England: European Bioinformatics Institute and Wellcome Trust Sanger Institute. Available at: www.ensembl.org/Canis_familiaris/index.html. Accessed May 24, 2009.

b. Entrez [database online]. Bethesda, Md: National Center for Biotechnology Information. Available at: www.ncbi.nlm.nih.gov/mapview/map_search.cgi?taxid=9615. Accessed May 24, 2009.

c. UCSC Genome Bioinformatics [database online]. Santa Cruz, Calif: University of California-Santa Cruz. Available at: genome.ucsc.edu. Accessed May 24, 2009.
d. Integrated DNA Technologies, Coralville, Iowa.
e. Wizard SV 96, Promega Corp, Madison, Wis.
f. United States Biochemical Corp, Cleveland, Ohio.
g. Applied Biosystems, Foster City, Calif.
h. Gene Codes Corp, Ann Arbor, Mich.
i. Ambion, Austin, Tex.
j. Superscript III, Invitrogen, Carlsbad, Calif.
k. Dako, Carpinteria, Calif.
l. Zymed Laboratories, Carlsbad, Calif.
m. Abcam, Cambridge, Mass.
n. Vector Laboratories Inc, Burlingame, Calif.
o. Fisher Scientific Research, Waltham, Mass.

References

1. Lust G. An overview of the pathogenesis of canine hip dysplasia. *J Am Vet Med Assoc* 1997;210:1443–1445.
2. Marschall Y, Distl O. Mapping quantitative trait loci for canine hip dysplasia in German Shepherd Dogs. *Mamm Genome* 2007;18:861–870.
3. Kaneene JB, Mostosky UV, Padgett GA. Retrospective cohort study of changes in hip joint phenotype of dogs in the United States. *J Am Vet Med Assoc* 1997;211:1542–1544.
4. Olsewski JM, Lust G, Rendano VT, et al. Degenerative joint disease: multiple joint involvement in young and mature dogs. *Am J Vet Res* 1983;44:1300–1308.
5. Carr AJ, Jefferson RJ, Benson MK. Joint laxity and hip rotation in normal children and in those with congenital dislocation of the hip. *J Bone Joint Surg Br* 1993;75:76–78.
6. Lust G, Beilman WT, Rendano VT. A relationship between degree of laxity and synovial fluid volume in coxofemoral joints of dogs predisposed for hip dysplasia. *Am J Vet Res* 1980;41:55–60.
7. Farese JP, Todhunter RJ, Lust G, et al. Dorsolateral subluxation of hip joints in dogs measured in a weight-bearing position with radiography and computed tomography. *Vet Surg* 1998;27:393–405.
8. Smith GK. Advances in diagnosing canine hip dysplasia. *J Am Vet Med Assoc* 1997;210:1451–1457.
9. Zhu L, Zhang Z, Feng F, et al. Single nucleotide polymorphisms refine QTL intervals for hip joint laxity in dogs. *Anim Genet* 2008;39:141–146.
10. Ramirez F, Dietz HC. Fibrillin-rich microfibrils: structural determinants of morphogenetic and homeostatic events. *J Cell Physiol* 2007;213:326–330.
11. Gupta PA, Putnam EA, Carmical SG, et al. Ten novel FBN2 mutations in congenital contractural arachnodactyly: delineation of the molecular pathogenesis and clinical phenotype. *Hum Mutat* 2002;19:39–48.
12. Todhunter RJ, Acland GM, Olivier M, et al. An outcrossed canine pedigree for linkage analysis of hip dysplasia. *J Hered* 1999;90:83–92.
13. Zhang Z, Zhu L, Sandler J, et al. Estimation of heritabilities, genetic correlations, and breeding values of four traits that collectively define hip dysplasia in dogs. *Am J Vet Res* 2009;70:483–492.
14. Gustafsson PO, Olsson SE, Kasstrom H, et al. Skeletal development of Greyhounds, German Shepherd Dogs and their crossbreed offspring. *Acta Radiol Suppl* 1975;344:81–108.
15. Smith GK, LaFond E, Gregor TP, et al. Within- and between-examiner repeatability of distraction indices of the hip joints in dogs. *Am J Vet Res* 1997;58:1076–1077.
16. Lust G, Williams AJ, Burton-Wurster N, et al. Joint laxity and its association with hip dysplasia in Labrador Retrievers. *Am J Vet Res* 1993;54:1990–1999.
17. Lust G, Todhunter RJ, Erb HN, et al. Repeatability of dorsolateral subluxation scores in dogs and correlation with macroscopic appearance of hip osteoarthritis. *Am J Vet Res* 2001;62:1711–1715.
18. Lust G, Todhunter RJ, Erb HN, et al. Comparison of three radiographic methods for diagnosis of hip dysplasia in eight-month-old dogs. *J Am Vet Med Assoc* 2001;219:1242–1246.
19. Todhunter RJ, Mateescu R, Lust G, et al. Quantitative trait loci for hip dysplasia in a cross-breed canine pedigree. *Mamm Genome* 2005;16:720–730.
20. Clark LA, Tsai KL, Steiner JM, et al. Chromosome-specific microsatellite multiplex sets for linkage studies in the domestic dog. *Genomics* 2004;84:550–554.
21. Mateescu RG, Burton-Wurster NI, Tsai K, et al. Identification of quantitative trait loci for osteoarthritis of hip joints in dogs. *Am J Vet Res* 2008;69:1294–1300.
22. Phavaphutanon J, Mateescu RG, Tsai KL, et al. Evaluation of quantitative trait loci for hip dysplasia in Labrador Retrievers. *Am J Vet Res* 2009;70:1094–1101.
23. Heath SC. Markov chain Monte Carlo segregation and linkage analysis for oligogenic models. *Am J Hum Genet* 1997;61:748–760.
24. Rozen S, Skaletsky H. Primer3 on the WWW for general users and for biologist programmers. *Methods Mol Biol* 2000;132:365–386.
25. Zhu L, Zhang Z, Friedenberg S, et al. The long (and winding) road to gene discovery for canine hip dysplasia. *Vet J* 2009;181:97–110.
26. Awano T, Katz ML, O'Brien DP, et al. A frame shift mutation in canine TPP1 (the ortholog of human CLN2) in a juvenile Dachshund with neuronal ceroid lipofuscinosis. *Mol Genet Metab* 2006;89:254–260.
27. Chase K, Lawler DF, Adler FR, et al. Bilaterally asymmetric effects of quantitative trait loci (QTLs): QTLs that affect laxity in the right versus left coxofemoral (hip) joints of the dog (*Canis familiaris*). *Am J Med Genet A* 2004;124A:239–247.
28. Putnam EA, Zhang H, Ramirez F, et al. Fibrillin-2 (FBN2) mutations result in the Marfan-like disorder, congenital contractural arachnodactyly. *Nat Genet* 1995;11:456–458.
29. Kealy RD, Lawler DF, Ballam JM, et al. Evaluation of the effect of limited food consumption on radiographic evidence of osteoarthritis in dogs. *J Am Vet Med Assoc* 2000;217:1678–1680.
30. Vanden Berg-Foels WS, Todhunter RJ, Schwager SJ, et al. Effect of early postnatal body weight on femoral head ossification onset and hip osteoarthritis in a canine model of developmental dysplasia of the hip. *Pediatr Res* 2006;60:549–554.
31. Jansen RC, Nap JP, Mlynárová L. Errors in genomics and proteomics. *Nat Biotechnol* 2002;20:19.
32. Pascal LE, True LD, Campbell DS, et al. Correlation of mRNA and protein levels: cell type-specific gene expression of cluster designation antigens in the prostate. *BMC Genomics* 2008;9:246.
33. Kielty CM, Baldock C, Lee D, et al. Fibrillin: from microfibril assembly to biomechanical function. *Philos Trans R Soc Lond B Biol Sci* 2002;357:207–217.
34. Chaudhry SS, Gazzard J, Baldock C, et al. Mutation of the gene encoding fibrillin-2 results in syndactyly in mice. *Hum Mol Genet* 2001;10:835–843.
35. Arteaga-Solis E, Gayraud B, Lee SY, et al. Regulation of limb patterning by extracellular microfibrils. *J Cell Biol* 2001;154:275–281.
36. Boregowda R, Paul E, White J, et al. Bone and soft connective tissue alterations result from loss of fibrillin-2 expression. *Matrix Biol* 2008;27:661–666.
37. Hurle JM, Corson G, Daniels K, et al. Elastin exhibits a distinctive temporal and spatial pattern of distribution in the developing chick limb in association with the establishment of the cartilaginous skeleton. *J Cell Sci* 1994;107:2623–2634.
38. Yanagino T, Yuasa K, Nagahama M, et al. Transcriptional regulation of fibrillin-2 gene by E2F family members in chondrocyte differentiation. *J Cell Biochem* 2009;106:580–588.
39. Toma DP, White KP, Hirsch J, et al. Identification of genes involved in *Drosophila melanogaster* geotaxis, a complex behavioral trait. *Nat Genet* 2002;31:349–353.
40. Walji AH. Some histological aspects of the hip joint capsule in the vervet monkey. *J Morphol* 1988;197:327–335.
41. Todhunter RJ, Lust G. Canine hip dysplasia: pathogenesis. In: Slatter D, ed. *Textbook of small animal surgery*. 3rd ed. St Louis: WB Saunders Co, 2003;2009–2019.
42. Greisen HA, Summers BA, Lust G. Ultrastructure of the articular

cartilage and synovium in the early stages of degenerative joint disease in canine hip joints. *Am J Vet Res* 1982;43:1963–1971.
43. Hui-Chou CS, Lust G. The type of collagen made by the articular cartilage in joints of dogs with degenerative joint disease. *Coll Relat Res* 1982;2:245–256.
44. Wiltberger H, Lust G. Ultrastructure of canine articular cartilage: comparison of normal and degenerative (osteoarthritic) hip joints. *Am J Vet Res* 1975;36:727–740.
45. Oda H, Igarashi M, Hayashi Y, et al. Soft tissue collagen in congenital dislocation of the hip. Biochemical studies of the ligamentum teres of the femur and the hip joint capsule. *Nippon Seikeigeka Gakkai Zasshi* 1984;58:331–338.
46. Jensen BA, Reimann I, Fredensborg N. Collagen type III predominance in newborns with congenital dislocation of the hip. *Acta Orthop Scand* 1986;57:362–365.
47. Wang EB, Zhao Q, Li LY, et al. Expression of COL1a1 and COL3a1 in the capsule of children with developmental dislocation of the hip [in Chinese]. *Zhongguo Dang Dai Er Ke Za Zhi* 2008;10:493–496.
48. Madsen JS. The joint capsule and joint laxity in dogs with hip dysplasia. *J Am Vet Med Assoc* 1997;210:1463–1465.
49. Steinetz BG, Williams AJ, Lust G, et al. Transmission of relaxin and estrogens to suckling canine pups via milk and possible association with hip joint laxity. *Am J Vet Res* 2008;69:59–67.
50. Samuel CS, Sakai LY, Amento EP. Relaxin regulates fibrillin 2, but not fibrillin 1, mRNA and protein expression by human dermal fibroblasts and murine fetal skin. *Arch Biochem Biophys* 2003;411:47–55.
51. Cardinet GH III, Guffy MM, Wallace LJ, et al. Canine hip dysplasia in German Shepherd Dog–Greyhound crossbreeds. *J Am Vet Med Assoc* 1983;182:393–395.
52. Matyas JR, Adams ME, Huang D, et al. Major role of collagen IIB in the elevation of total type II procollagen messenger RNA in the hypertrophic phase of experimental osteoarthritis. *Arthritis Rheum* 1997;40:1046–1049.
53. Hirokawa N, Noda Y. Intracellular transport and kinesin superfamily proteins, KIFs: structure, function, and dynamics. *Physiol Rev* 2008;88:1089–1118.
54. Sutter NB, Bustamante CD, Chase K, et al. A single IGF1 allele is a major determinant of small size in dogs. *Science* 2007;316:112–115.

Appendix 1

Primer sequences for amplification of *FBN2*, *FBN1*, and *GPI* (glucose phosphate isomerase) mRNA from hip joint capsule tissue of dogs.

Gene	Location	Forward primers	Reverse primers
FBN2	Exon 4-5	CAGTGCCAGAAGGGATATATTGGAA	CGTCCACCATTCTGACATCCATTT
FBN2	Exon 30-31	TGGCTTCATGGCTTCAATGGA	CTCACATTCCCCAAACATACAGATGT
FBN2	Exon 59-60	GCTATGTCCTACAAGAGGATGCAAA	GCAGTTGTGTTGTTTGGTTTGACA
GPI	Exon 2-3	ACACCGTGATGCAGATGCT	TGATCTTCTCGCCACTGAACATG
FBN1	Exon 6-7	GCCGAGGCTTCATTCCAAATATC	GGGATGGCCTGGCATTCAT

Appendix 2

FBN2 primer sequences for exon amplification to test for alternative transcripts in a study of hip dysplasia in dogs.

Primer location	Direction	Sequence	Expected amplicon size (bp)
Exon 26	Forward	aggctacgaaagtgggttca	—
Exon 28	Reverse	ttcatagctgccttcggaat	364
Exon 29	Reverse	gtacattggccaccatcaca	468
Exon 30	Reverse	gttctcacattccccaaaca	598
Exon 31	Reverse	gtgggcaccaatttcacact	697
Exon 33	Reverse	ttgatgttttctgcgcactc	942
Exon 34	Forward	gtgcatatcgttgcgagtgt	—
Exon 36	Reverse	acacagaggccattcacaca	235
Exon 37	Reverse	cgaggtccgaacttcaggta	349
Exon 39	Reverse	cctggtaactcctggcattc	568
Exon 40	Reverse	atacaccagggtgtgcgaaa	699
Exon 41	Reverse	cgttctcacaagtggttccat	846
Exon 42	Reverse	ggatgtcaaaggtgaatccag	996
Exon 43	Reverse	accaggagcaggtcgttgta	1,132

— = Not applicable.

Appendix 3

Haplotype structure of intron 30 of *FBN2* where a deletion mutation occurred, in dogs with CHD.

Haplotype structure	Sequence		Sequence	Sequence		Sequence		Sequence	Sequence	Sequence	Sequence
Unaffected homozygous	…CATCT	G	TGCAC…	GGGAA	A	GAGGCTTT	T	TCAGT…	AGATTA	TACTTA	ACTTTTA…
Affected homozygous	…CATCT	A	TGCAC…	GGGAA	G	GAGGCTTT	C	TCAGT…	AGATTA	::::::	ACTTTTA…
Heterozygous	…CATCT	R	TGCAC…	GGGAA	R	GAGGCTTT	Y	TCAGT…	AGATTA	NNNNN	ACTTTTA…
Base position		41			68		77			189–195	

N = Unknown nucleotide sequence.